**MASPEC-D-24-00018 Submitted to IJMS special issue honoring Prof. Mary T. Rodgers.**
**Guest editors: Dr. Zhibo Yang and Professor Yu Y. Xia.**

**Revised Version: 27 March 2024**

# Competition Between Transmetalation and Electron Transfer in the Gas-phase Reactions of Ytterbium Complex Trications and the Tetraphenylborate Anion.[ξ]

Weam A. O. Altalhi,[a,b] Kimberly C. Fabijanczuk,[c] Allan J. Canty,[d]
Scott A. McLuckey,[*,c] and Richard A. J. O'Hair[*, a]

a. School of Chemistry and Bio21 Institute of Molecular Science and Biotechnology, The University of Melbourne, Victoria 3010, Australia
b. Department of Chemistry, Prince Sattam Bin Abdulaziz University, Hotat Bani Tamim, 16511 Saudi Arabia
c. Department of Chemistry, Purdue University, West Lafayette, Indiana 47907-2084, United States of America.
d. School of Physical Sciences - Chemistry, University of Tasmania, Private Bag 75, Hobart, Tasmania 7001, Australia.

**Abstract:**
Gas-phase ion-ion reactions between the trication, $[Yb(L)_3]^{3+}$ (where L = N,N,N',N'-tetramethylpyridine-2,6-dicarboxamide), and the tetraphenylborate anion, $[BPh_4]^-$, and its sodium bound dimer, $[(BPh_4)_2Na]^-$, were examined to establish whether ion-pair formation and transmetalation from boron to ytterbium can occur. Ion clusters that were formed with the formal +3 oxidation state for the ytterbium metal centre include: the ion pair $[Yb^{(III)}(L)_3][BPh_4]^{2+}$ (*m/z* 578, (**6a**)); the ion triplet $[Yb^{(III)}(L)_3][BPh_4]_2^+$ (*m/z* 1475, (**7a**)); and $[Yb^{(III)}(L)_3(BPh_4)_3Na]^+$ (*m/z* 1817, (**8a**)). In addition, electron transfer from $[BPh_4]^-$ to $[Yb(L)_3]^{3+}$ resulted in complexes in which the the ytterbium metal centre is in the formal +2 oxidation state, which reacted further to yield the ion pairs: $[Yb^{(II)}(L)_3][BPh_4]^+$ (*m/z* 1156, (**7b**)); $[Yb^{(II)}(L)_2][BPh_4]^+$ (*m/z* 935, (**8b**)); and $[Yb^{(II)}(L)][BPh_4]^+$ (*m/z* 714, (**9b**)). Selected ion pairs were mass isolated and subjected to collision-induced dissociation (CID) to examine if they underwent transmetalation from B to Yb. Most of the observed ytterbium(III) complexes were found to undergo transmetalation. Density functional theory (DFT) calculations were used to determine the energetics for the sequential ion-ion reactions associated with the formation of $[Yb^{(II)}(L)_2][BPh_4]^+$ as well as its fragmentation reactions via ligand loss (observed experimentally) versus transmetalation (not observed experimentally).

## 1. Introduction

In recent years there has been a renewed interest in the chemistry of the lanthanides, driven by their unique electronic properties and potential applications in organic

[ξ] Dedicated with respect and admiration to Prof. Mary T. Rodgers on the occasion of her 60th Birthday and in recognition of her important contributions to gas-phase ion chemistry and service our community.

synthesis[1-3] and materials science.[4] While there has been significant progress in the study of ytterbium chemistry of relevance to organic chemistry, challenges remain. For example, some structural and mechanistic aspects of ytterbium organometallic chemistry remain poorly understood. A case in point are the *pseudo*-Grignards first described by Evans and co-workers over 50 years ago.[5, 6] They reported that ytterbium metal reacts with alkyl and aryl iodides in tetrahydrofuran (THF) at low temperatures to give solutions of "(R)YbI(S)$_n$" (where S = solvent), which undergo typical Grignard type reactions. Subsequent work has suggested that these are +2/+3 mixed valence species, but isolation and structural characterisation of these compounds has been challenging due to a combination of factors, including the existence of Schlenk equilibria, redox processes, the role of coordinated solvent (S), and the thermal lability of the Yb–C σ-bond. Four decades after Evan's report, Wiecko *et al.* isolated two different crystalline materials from a ''(Ph)YbI(thf)$_n$'' mixture and showed that they corresponded to [(Ph)$_3$Yb$^{(III)}$(thf)$_3$] and [Yb$^{(II)}$I$_2$(thf)$_4$].[7, 8] By changing the solvent to the bidentate dimethoxyethane (dme), they isolated the charge separated mixed valence ion pair [{Yb$^{(II)}$(dme)$_4$}{(Ph)$_4$Yb$^{(III)}$(dme)}$_2$].

Apart from oxidative addition of alkyl or aryl halides to ytterbium metal, a range of other approaches to the stoichiometric and *in situ* formation of organoytterbium species have been reported.[9-11] For example, transmetalation reactions, which involve the transfer of carbon ligands (e.g., alkyl and aryl) from one metal to another,[12] have been used to prepare organoytterbium complexes that are either neutral or with a formal negative charge at ytterbium ("ate" complexes)[13] from ytterbium(III) salts and organolithium or organomagnesium compounds and these have been structurally characterised[14-16] or have been implicated in reactions with organic substrates.[17-20] Fewer transmetalation reactions of ytterbium salts with other organometallic reagents have been reported. While the tetraphenylborate anion undergoes transmetalation to a wide range of transition metal salts,[21] its reactions with ytterbium salts have solely been used to form a range of complexes suitable for X-ray crystallography.[22] The types of complexes that have been isolated have ranged between discrete ionic complexes such as [Yb(18-cr-6)(NCMe)$_3$][BPh$_4$]$_2$ and [(C$_6$F$_5$)Yb(thf)$_5$][BPh$_4$][22, 23] through to complexes such as **1** - **3** (Scheme 1, A)[24-26] which have been described as *pseudo*-metallocenes since the tetraphenylborate acts as a coordinating ligand.[22]

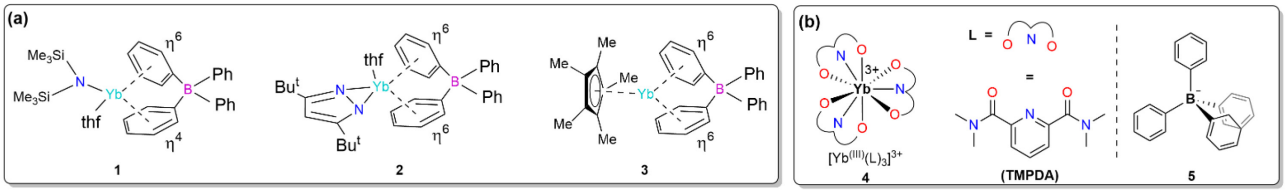


**Scheme 1:** (a) examples of structures of ytterbium tetraphenylborate pseudo-metallocenes determined via X-ray crystallography; (b) ion–ion reactions in the gas-phase between the ytterbium trication (**4**) and tetraphenylborate (**5**) to directly probe the role of ion pairs in transmetalation (this work).

As part of a series of studies aimed at examining fundamental aspects of transmetalation,[27-29] we recently described a new mass-spectrometry based approach deploying gas-phase ion-ion reactions.[30, 31] We found that reactions between tris-1,10-phenanthroline metal dications, [(phen)$_3$M]$^{2+}$ (where M = Ni or Mg), and the tetraphenylborate anion yielded the ion pairs [M$^{(II)}$(phen)$_3$][BPh$_4$]$^+$, which underwent

transmetalation upon loss of a phen ligand to give the organometallic complexes $[(Ph)M(phen)_2]^+$.[32] Here we examine the first ion-ion reactions between a ytterbium trication and the tetraphenylborate anion, **(5)** (Scheme 1, B) and its sodium bound dimer, $[(BPh_4)_2Na]^-$ **($Na^+.5_2$)**, with the aim of establishing whether ion pair formation and transmetalation can occur in these systems. Specifically, $[Yb(L)_3]^{3+}$ **(4)** (where L = *N,N,N',N'*-tetramethylpyridine-2,6-dicarboxamide TMPDA) was chosen, since this class of ytterbium trications are well established species in both the condensed phase[33, 34] and the gas phase.[35]

## 2. Experimental

### 2.1. Materials

Ytterbium$^{(III)}$ nitrate pentahydrate and sodium tetraphenylborate were both purchased from Millipore Sigma (St. Louis, MO). HPLC-grade methanol (MeOH) was purchased from Fisher Scientific (Pittsburgh, PA). *N,N,N',N'*-tetramethylpyridine-2,6 dicarboxamide (TMPDA) was synthesised as reported.[36]

### 2.2. Sample Preparation

Ytterbium$^{(III)}$ nitrate pentahydrate (Yb) was dissolved into MeOH at an initial concentration of 2.2 mM. Purified TMPDA was dissolved into MeOH at an initial concentration of ~4.5 mM. Stock solution of each Yb and TMPDA were used to prepare a final mixed solution of Yb and TMPDA, ~20 and 40 µM, respectively. It was found empirically that a 1:2 molar ratio yielded the most stable and consistent metal complex. Sodium tetraphenylborate ($NaBPh_4$) was dissolved into MeOH at an initial concentration of ~3 mM and diluted to a final concentration of 50 µM.

### 2.3. Mass Spectrometry

All experiments were conducted on a Sciex QqTOF 5600 platform that has been previously modified to enable the study of gas-phase ion-ion reactions.[37] A dual pulsed nano-electrospray ionisation (ESI) spray system was used to generate anions and cations separately.[38] First, $[Yb^{(III)}(L)_3]^{3+}$ was generated via positive nano-ESI, mass selected (isolated at ~0.3 unit resolution), and transferred to the high pressure collision cell, q2. Second, $[BPh_4]^-$ was generated via negative nano-ESI, mass selected in Q1 (isolated at unit resolution) and transferred to q2 where auxiliary AC waveforms were applied for 50 ms (timing for all ion-ion reactions unless specified elsewhere) for mutual trapping of oppositely charged ions allowing for ion-ion reactions to occur at a low mass cut-off of 100. Subsequent products were isolated and subjected to single-frequency ion trap collision induced dissociation (CID) at q=0.2 for further interrogation prior to transmission to the time-of-flight tube for mass analysis.[39]

### 2.4. DFT calculations

Density Functional Theory (DFT) with Gaussian 16 (G16) was employed[40]to fully optimize the structures at the M06 level of theory.[41] For describing the Yb, the SDD basis set was chosen while the 6-31G(d) basis set was used for all other atoms. All the frequency calculations were calculated using the same level of theory as those for the optimisation process and were used to confirm the local minima (no imaginary frequencies). The Conformer–Rotamer Ensemble Sampling Tool (CREST) (version

2.11) was utilised to search for the conformers of the tetraphenylborate dimer dianion $[(BPh_4)_2]^{2-}$.[42] Using the search tool with semiempirical tight-binding model -gfn2 as the level of theory[43] and in the gas-phase (no implicit solvation was added), three conformers of $[(BPh_4)_2]^{2-}$ were found. The three conformers were then optimised via DFT using M06 level of theory and 6-31G(d) basis set. This basis set combination is referred as **BS1**. The three structures were further refined, and single point energy calculations carried out with the basis set wB97XD def2tzvp/**BS2**. The enthalpy at 0 K, $H^0$, of each species was obtained using wB97XD def2tzvp/**BS2**.

## 3. Results and Discussion

### 3.1. Product channels in the ion-ion reaction between $[Yb^{(III)}(L)_3]^{3+}$ (4) and $[BPh_4]^-$ (5).

Positive ion nano electrospray ionisation (+nESI) of a methanolic solution containing 20 μM $Yb(NO_3)_3.5H_2O$ and 40 μM *N,N,N',N'*-tetramethylpyridine-2,6-dicarboxamide (TMPDA = L) gave rise to an abundant signal of the desired triply charged cation $[Yb^{(III)}(L)_3]^{3+}$ **(4)** at *m/z* 279, which was mass selected and injected into the ion trap for ion-ion reactions (Yb has seven stable isotopes and in all cases the most abundant peak was mass selected, which is dominated by the $^{174}Yb$ isotope). Negative ion nano-electrospray ionisation (-nESI) of a 50 μM methanolic solution of sodium tetraphenylborate gave rise to an abundant signal of the singly charged anion $[BPh_4]^-$ **(5)** at *m/z* 319, which was mass selected and injected into the ion trap. Ion-ion reactions were enabled by mutually storing **(4)** and**(5)** in the ion trap for 50 ms, resulting in the positive ion mass spectrum shown in Figure 1A.

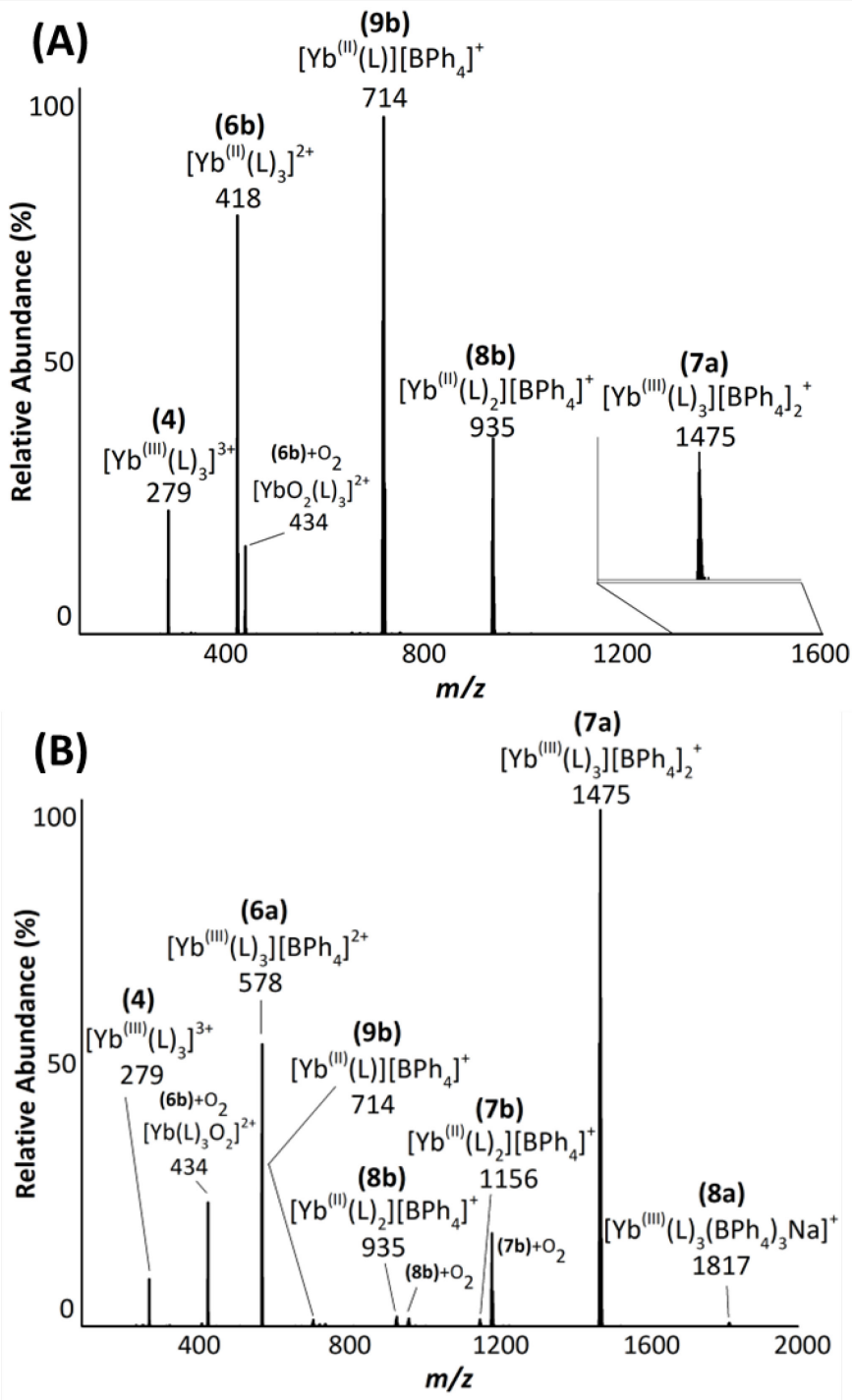


**Figure 1:** (A) Ion-ion mass spectrum of $[Yb^{(III)}(L)_3]^{3+}$ (**4**) at *m/z* 279 with $[BPh_4]^-$ (**5**) at *m/z* 319, showing the formation of the ion triplet $[Yb^{(III)}(L)_3][BPh_4]^{2+}$ (**7a**) at *m/z* 1475; (B) ion-ion mass spectrum of $[Yb^{(III)}(L)_3]^{3+}$ (**4**) at *m/z* 279 with $[(BPh_4)_2Na]^-$ (**$Na^+.5_2$**) at *m/z* 661 showing the formation of the ion triplet $[Yb^{(III)}(L)_3][BPh_4]^{2+}$ (**7a**) at *m/z* 1475 and the ion pair $[Yb(III)(L)_3][BPh_4]^{2+}$ (**6a**) at *m/z* 578. Oxygen containing product ions arise from ion-molecule reactions with background oxygen.

Although the spectrum contains a range of different product ions, they can be rationalised as arising from two primary ion-ion reaction channels (Scheme 2): formation of the ion pair $[Yb^{(III)}(L)_3][BPh_4]^{2+}$ **(6a)** at *m/z* 578 (eq. 1a), which was not observed in our initial experiments (shown in Figure 1A), as well as

$[Yb^{(II)}(L)_3]^{2+}$ **(6b)** at *m/z* 418 via an electron transfer pathway (eq. 1b). A plausible explanation for the observation of the ion triplet $[Yb^{(III)}(L)_3][BPh_4]_2^+$ **(7a)** [44] at *m/z* 1475 is that it arises from a second ion-ion reaction between the ion pair **(6a)** and **(5)** (eq. 2a). The $Yb^{(II)}$ complex **(6b)** also undergoes a second ion-ion reaction with **(5)** to yield the ion pair resulting from loss of a ligand $[Yb^{(II)}(L)_2][BPh_4]^+$ **(8b)** at *m/z* 935 (eq. 2b) which can lose a second ligand to give $[Yb^{(II)}(L)][BPh_4]^+$ **(9b)** at *m/z* 714 (eq. 3b). The ion at *m/z* 434, which we assign as $[YbO_2(L)_3]^{2+}$, appears to arise from an ion-molecule reaction between $[Yb^{(II)}(L)_3]^{2+}$ and background oxygen. In addition, there are several other product ions in Figure 1B that contain oxygen. There are other examples of ion-molecule reactions between background oxygen and ions, including the reactions peptide radical cation ETD products with $O_2$,[25] reactions of distonic radical cations with $O_2$,[26] reactions of molybdenum halide cluster anions with oxygen or water.[27] Due to the high oxophilicity of ytterbium,[45] there are several examples of ytterbium complexes reacting with adventitious oxygen in the condensed phase to form peroxides.[46-48] While the exact nature of the bonding within the oxygen containing species in our experiments is unclear, of all the oxygen reduced species (superoxide from 1e reduction, peroxide from 2e reduction or oxide formation via 4e reduction), superoxide complexes seem most likely as they would result in ytterbium complexes in the common +3 formal oxidation state. Perhaps gas-phase IR spectroscopy could shed further insights into the bonding arrangements in these complexes.[49]

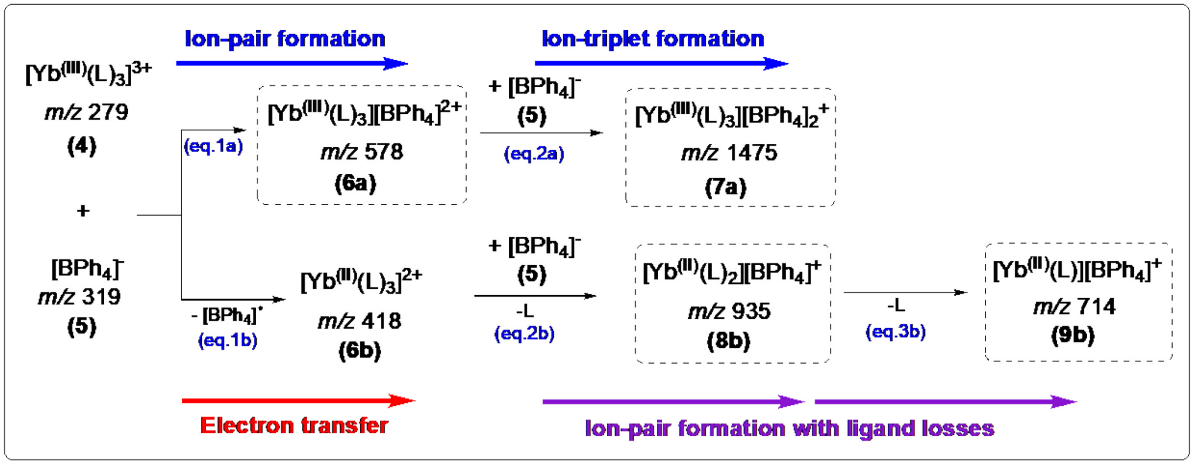


**Scheme 2:** Sequential ion-ion reactions between $[Yb^{(III)}(L)_3]^{3+}$ (**4**) and $[BPh_4]^-$ (**5**) that give rise to the primary and secondary product ions (Figure 1, A). Species shown in dashed boxes were further examined to establish whether they underwent transmetalation.

### 3.2. Why did the ion pair $[Yb^{(III)}(L)_3][BPh_4]^{2+}$ (6a) initially elude detection?

As noted, the ion $[Yb^{(III)}(L)_3][BPh_4]^{2+}$ (**6a**) at *m/z* 578 formed via eq.1a (Scheme 2) was not initially observed in the full mass spectrum (Figure 1A). We postulated that there are two possible reasons: (1) (**6a**) is unstable and that $[Yb^{(III)}(L)_3]^{3+}$ (**1**) instead reacts directly with the dimer dianion $[(BPh_4)_2]^{2-}$ (which has the same *m/z* value as $[BPh_4]^-$) to give the ion triplet $[Yb^{(III)}(L)_3][BPh_4]_2^+$ (**7a**) – this reaction does not require formation

of (**6a**) as an intermediate; (2) $[Yb^{(III)}(L)_3][BPh_4]^{2+}$ (**6a**) rapidly undergoes a second ion-ion reaction with another tetraphenylborate anion to give (**7a**).

### 3.2.1. Testing hypothesis 1:

Hypothesis 1 requires that: (i) (**6a**) is an unstable reactive intermediate in the gas-phase; and (ii) $[(BPh_4)_2]^{2-}$ be a stable reactive intermediate in the gas-phase. To test point (i), we examined whether (**6a**) could be formed in the ion-ion reaction experiment between $[Yb^{(III)}(L)_3]^{3+}$ (**4**) and tetraphenylborate sodium bound $[(BPh_4)_2Na]^-$ (**$Na^+.5_2$**). An examination of Figure 1B reveals the formation of previously observed ions (**7a**), (**8b**) and (**9b**). Interestingly, the missing $[Yb^{(III)}(L)_3][BPh_4]^{2+}$ (**6a**) at *m/z* 578 was now detected, highlighting that it is a stable species in the gas phase. Other ions observed include the ion pair $[Yb^{(II)}(L)_3][BPh_4]^+$ (**7b**) at *m/z* 1156 (Scheme 3, eq. 5b) and $[Yb^{(III)}(L)_3(BPh_4)_3Na]^+$ (**8a**) at *m/z* 1817 (Scheme 3, eq. 5a) as well as various ions arising from addition of background oxygen.

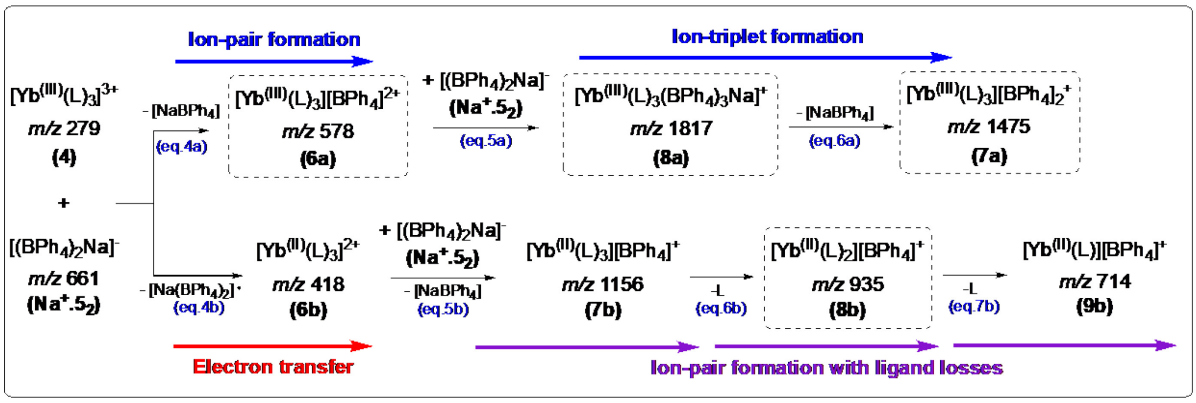


**Scheme 3:** Sequential ion-ion reactions between $[Yb^{(III)}(L)_3]^{3+}$ (**4**) and $[(BPh_4)_2Na]^-$ (**$Na^+.5_2$**) that give rise to the primary and secondary product ions (Figure 1, B). Species shown in dashed boxes were further examined to establish whether they underwent transmetalation.

Regarding point (ii), this is not only a key issue for our study, but fundamentally important in inorganic chemistry as it relates to the well-known concept of phenyl embraces,[28] which are often observed in the X-ray crystallography of salts formed by the tetraphenylphosphonium cation, $[PPh_4]^+$ [29] and the tetraphenylborate anion, $[BPh_4]^-$.[30] Although we could find no experimental evidence for $[(BPh_4)_2]^{2-}$ in the gas phase (there were no peaks spaced at m/z 0.5 for the isotopes), to test whether the tetraphenylborate dimer dianion $[(BPh_4)_2]^{2-}$ is stable in the gas phase, we utilised DFT calculations to calculate the energy of dissociation into two $[BPh_4]^-$ monomers (eq. 8). DFT results predicted that all four calculated conformers of the dianion $[(BPh_4)_2]^{2-}$ were not stable in the gas-phase (Figure S5).

$$[(BPh_4)_2]^{2-} \rightarrow 2\,[BPh_4]^- \quad \text{(eq. 8)}$$

### 3.2.2. Testing hypothesis 2:

Having established that $[Yb^{(III)}(L)_3][BPh_4]^{2+}$ (**6a**) is a stable reactive intermediate in the gas-phase whereas $[(BPh_4)_2]^{2-}$ is not, we then revisited the ion-ion reaction conditions to confirm that the ion triplet $[Yb^{(III)}(L)_3][BPh_4]_2^{+}$ (**7a**) is formed via sequential reactions (Scheme 2) from firstly reacting (**4**) with (**5**) via eq.1a to form (**6a**) followed by another ion-ion reaction of (**6a**) with (**5**) to give (**7a**) (eq.2a). We first varied the reaction time. At a reaction time of 200 ms (Figure S1, A), the formation of $[Yb^{(III)}(L)_3][BPh_4]^{2+}$ (**6a**) at *m/z* 578 and $[Yb^{(III)}(L)_3][BPh_4]_2^{+}$ (**7a**) is observed together with the formation of other ytterbium ions as described previously. Increasing the reaction time to 400 ms only results in a decrease in the relative abundance of $[Yb^{(III)}(L)_3]^{3+}$ (**4**) (Figure S1, B). In another type of experiment, the initially formed ion $[Yb^{(III)}(L)_3][BPh_4]^{2+}$ (**6a**) at *m/z* 578 was selectively removed during the experiment, preventing it from undergoing a second ion-ion reaction with another tetraphenylborate anion. The ion triplet $[Yb^{(III)}(L)_3][BPh_4]_2^{+}$ (**7a**) disappeared (Figure S1, C), highlighting that (**7a**) is indeed formed via the sequential reaction (eq, 2a, Scheme 2).

### 3.3. The search for transmetalation from B to Yb: role of oxidation state of Yb and number of ligands.

Selected ion pairs that were formed in the ion-ion reactions (Figure 1, Schemes 2 and 3) were mass selected and subjected to CID to examine if they could undergo transmetalation (Figure 2, Scheme 4).

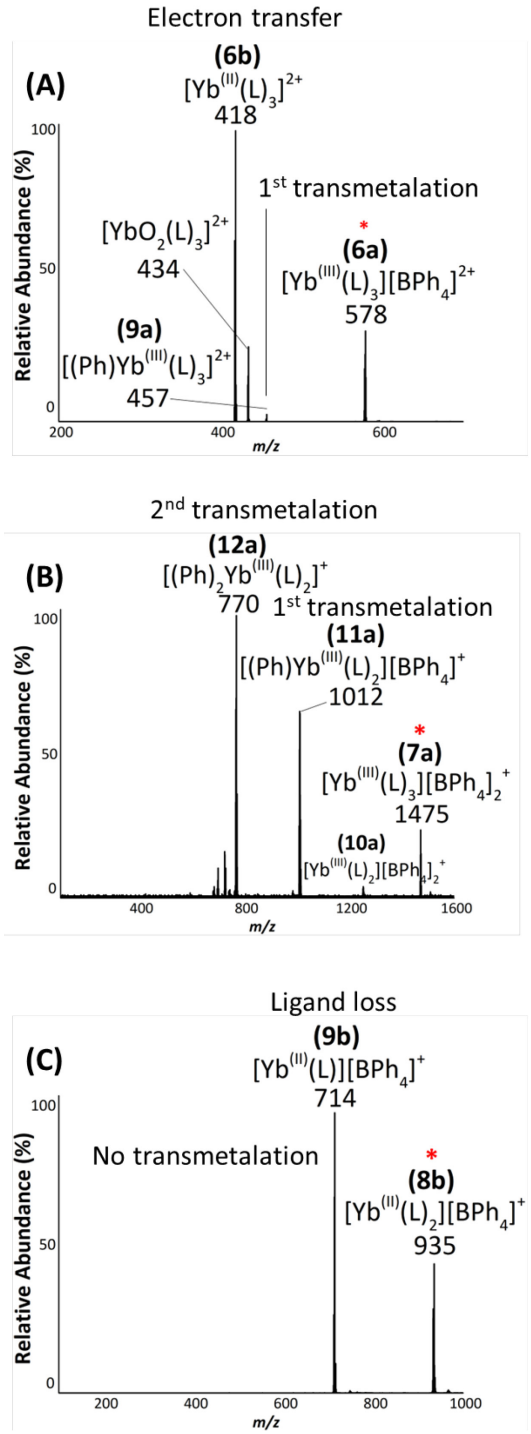


**Figure 2:** CID of the: (A) ion pair $[Yb^{(III)}(L)_3][BPh_4]^{2+}$ (*m/z* 578, (**6a**), 50mV for 50ms); (B) ion triplet $[Yb^{(III)}(L)_3][BPh_4]_2^{+}$ (*m/z* 1475, (**7a**) , 140mV for 100ms);); (C) ion pair $[Yb^{(II)}(L)_2][BPh_4]^{+}$ (*m/z* 935, (**8b**) , 45mV for 50ms);). The red asterisk indicates the mass selected precursor ion subjected to CID.

### 3.3.1 $[Yb^{(III)}(L)_3][BPh_4]^{2+}$ (*m/z* 578, (6a))

The main fragmentation channel in the CID spectrum of the mass selected ion pair $[Yb^{(III)}(L)_3][BPh_4]^{2+}$ (**6a**) (Figure 2A and Scheme 4A) involves formation of $[Yb^{(II)}(L)_3]^{2+}$ (**6b**) at *m/z* 418 via electron transfer (eq. 9b). A minor loss of triphenylboron is observed. This may arise via transmetalation to give the organometallic ion

$[(Ph)Yb^{(III)}(L)_3]^{2+}$ (**9a**) at *m/z* 457 (eq.9a), although we cannot rule out phenide transfer to one of the coordinated ligands, L.

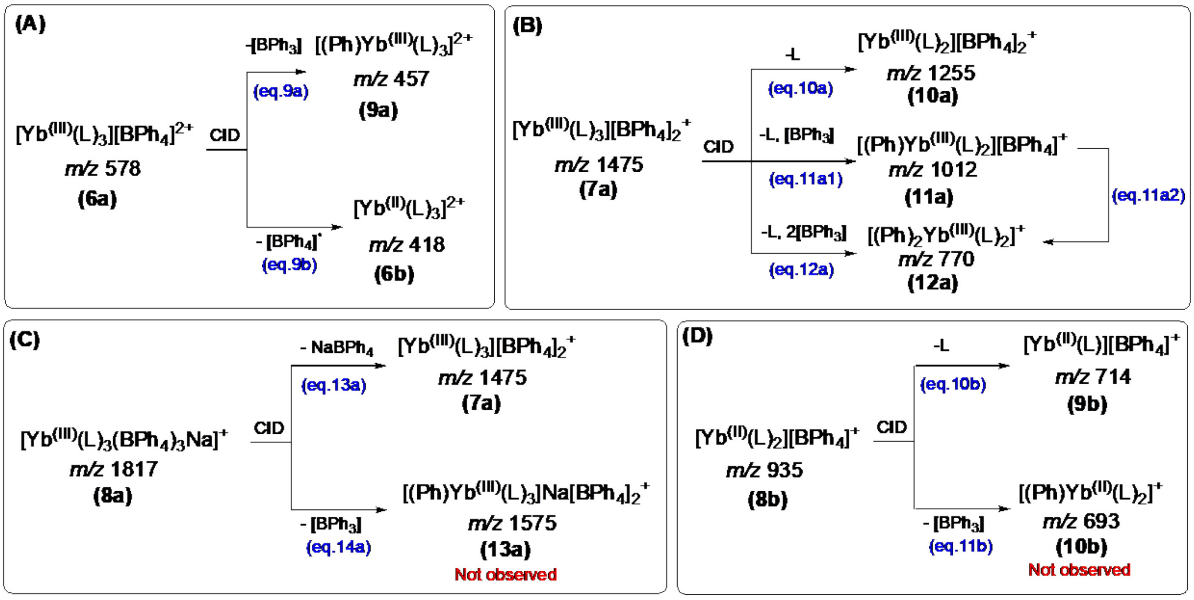


**Scheme 4:** Summary of fragmentation reactions of the ion pairs: (A) $[Yb^{(III)}(L)_3][BPh_4]^{2+}$ (*m/z* 578, (**6a**)); (B) $[Yb^{(III)}(L)_3][BPh_4]_2^+$ (*m/z* 1475, (**7a**)); (C) $[Yb^{(III)}(L)_3(BPh_4)_3Na]^+$ (*m/z* 1817, (**8a**)); (D) $[Yb^{(II)}(L)_2][BPh_4]^+$ (*m/z* 935, (**8b**)).

### 3.3.2 $[Yb^{(III)}(L)_3][BPh_4]_2^+$ (*m/z* 1475, (7a))

The CID spectrum of the ion triplet $[Yb^{(III)}(L)_3][BPh_4]_2^+$ (**7a**) (Figure 2B and Scheme 4B) shows the formation of $[Yb^{(III)}(L)_2][BPh_4]_2^+$ (**10a**) at *m/z* 1255 via ligand loss (eq. 10a) and $[(Ph)Yb^{(III)}(L)_2][BPh_4]^+$ (**11a**) at *m/z* 1012 (eq. 11a1) which is formed via ligand loss and transmetalation. A second transmetalation reaction was also observed from (**11a**) to give $[(Ph)_2Yb^{(III)}(L)_2]^+$ (**12a**) at *m/z* 770 (eq. 12a). This was confirmed by applying CID on the isolated ion (**11a**) to give $[(Ph)_2Yb^{(III)}(L)_2]^+$ (**12a**) at *m/z* 770 (eq. 11a2) (Figure S2).

### 3.3.3 $[Yb^{(III)}(L)_3(BPh_4)_3Na]^+$ (*m/z* 1817, (8a))

The fragmentation pattern of (**8a**) solely shows a loss of $NaBPh_4$ (eq. 13a, Figure S3) to give the ion triplet $[Yb^{(III)}(L)_3][BPh_4]_2^+$ (**7a**) (Figure S3 and Scheme 4C). No transmetalation reaction was observed (eq. 14a). Loss of $NaBPh_4$ is also observed in the CID spectrum of the sodium bound dimer, $[(BPh_4)_2Na]^-$ **($Na^+.5_2$)** (Figure S4).

### 3.3.4 $[Yb^{(II)}(L)_2][BPh_4]^+$ (*m/z* 935, (8b))

Applying CID to the ion pair $[Yb^{(II)}(L)_2][BPh_4]^+$ **(8b)** only results in the formation of $[Yb^{(II)}(L)][BPh_4]^+$ **(9b)** at *m/z* 714 (Figure 2C and Scheme 4D). No transmetalation occurs since the ion $[Yb^{(II)}(L)_2(Ph)]^+$ **(10b)** at *m/z* 693 was not observed (eq. 11b).

## 3.4. DFT calculations of selected reactions.

To gain a better understanding of these reactions, DFT methods were employed to calculate the energies associated with the formation of some of the observed ytterbium

complexes. Attempts were made to calculate the transmetalation pathways and the ligand loss pathways. The formation of $[Yb^{(II)}(L)_3]^{2+}$ (**6b**) from the reaction between (**4**) and (**5**) via electron transfer (eq.1b, Scheme 2) was calculated to be exothermic by -152.2 kcal/mol. The addition of an anion $[BPh_4]^-$ to (**6b**) via (eq.2b, Scheme 2) to give $[Yb^{(II)}(L)_2][BPh_4]^+$ (**8b**) with a loss of a ligand was calculated to be exothermic by -69.1 kcal/mol. Both of these results are consistent with the experimental observation of these reactions under the ion-ion reaction conditions of the ion trap mass spectrometer. The ion pair (**8b**) lost a ligand under CID conditions to give $[Yb^{(II)}(L)][BPh_4]^+$ (**9b**) and this process was calculated to be endothermic by +30.6 kcal/mol (Figure 4). On the other hand, the ion pair $[Yb^{(II)}(L)_2][BPh_4]^+$ (**8b**) did not fragment under CID conditions to give the organometallic ion $[(Ph)Yb^{(II)}(L)_2]^+$ (**10b**) via transmetalation even though this process was calculated to be endothermic by +26.5 kcal/mol. Although we have not been able to locate the transmetalation transition state, it seems likely that the barrier is higher than the energy required for ligand loss to give $[Yb^{(II)}(L)][BPh_4]^+$ (**9b**).

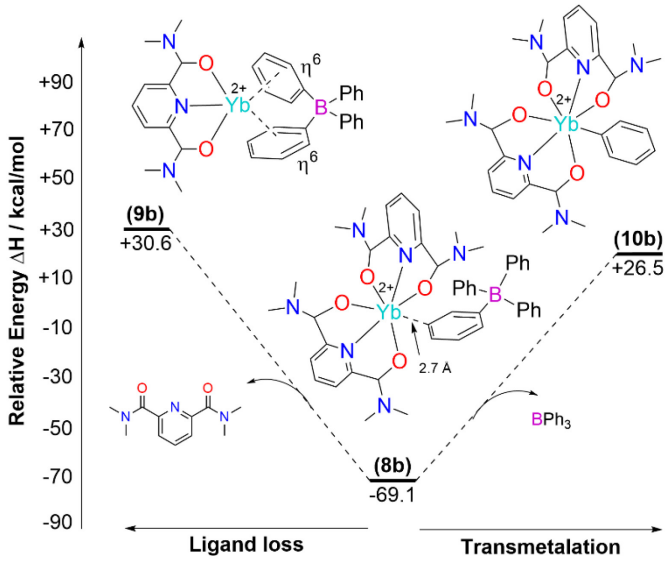


**Figure 4:** DFT calculations estimating the thermodynamics of transmetalation and ligand loss pathways from $[Yb^{(II)}(L)_2][BPh_4]^+$ (**8b**) to give $[Yb^{(II)}(L)][BPh_4]^+$ (**9b**) (left) and $[(Ph)Yb^{(II)}(L)_2]^+$ (**10b**) (right). The energies are ΔH° in the gas-phase obtained at the M06/SDD-6-31G(d) level of theory.

## 4. Conclusions

In conclusion, ion-ion reactions between the ytterbium trication, $[Yb^{(III)}(L)_3]^{3+}$ (**4**) and the tetraphenylborate anion (**5**), or its sodium bound dimer (**$Na^+.5_2$**), provide fundamental information on the competition between electron transfer pathways and ion-pair formation, together with information on which ion pairs can undergo further reaction via transmetalation. In the case of the reaction between (**4**) and (**5**), electron transfer dominates (Figure 1a, eq. 1b of Scheme 2) to produce the ytterbium dication, $[Yb(L)_3]^{2+}$ (**6b**) which undergoes a second ion-ion reaction with (**5**) via ligand displacement reaction to give the ion pairs $[Yb^{(II)}(L)_2][BPh_4]^+$ (**8b**) and $[Yb^{(II)}(L)][BPh_4]^+$ (**9b**) (eqs. 2b and 3b of Scheme 2). The former ion pair does not undergo transmetalation, preferring ligand loss. In contrast, when (**4**) is allowed to react with the sodium bound dimer, (**$Na^+.5_2$**), electron transfer is suppressed and becomes a

minor channel (Figure 1b, Scheme 3). Since loss of $NaBPh_4$ allows any excess energy of the ion-ion reaction to be carried away, abundant ion pairs are observed for $[Yb^{(III)}(L)_3][BPh_4]^{2+}$ (**6a**) and $[Yb^{(III)}(L)_3][BPh_4]_2^{+}$ (**7a**) (eqs 4a and 6a of Scheme 3). The former ion pair undergoes direct transmetalation while the latter undergoes transmetalation with concomitant ligand loss. When establishing that the sequential ion-ion reactions between (**4**) and (**5**) gives rise to $[Yb^{(III)}(L)_3][BPh_4]_2^{+}$ (**7a**), it was important to rule out that $[(BPh_4)_2]^{2-}$, which is isobaric with respect to (**5**), is unstable in the gas-phase. DFT calculations reveal that various conformers of the tetraphenylborate dimer dianion are indeed thermodynamically unstable in the gas-phase. This is consistent with the study of D'Oria et al. who found that the tetraphenylphosphonium dimer dication $[(PPh_4)_2]^{2+}$ is unstable.[31] Thus, it appears that a key stabilising factor that facilitates the various phenyl embraces observed in the solid state are the attractive forces of the counter anions (which are absent in the gas-phase), which offset the repulsive forces of the like charges (anion-anion in $[(BPh_4)_2]^{2-}$ or cation-cation $[(PPh_4)_2]^{2+}$).

## Author Contributions

W.A.O.A. carried out the DFT calculations, collated and checked all the DFT data, and contributed to manuscript preparation. K.C.F. identified and optimised routes to the gas-phase formation Yb complexes, carried out the ion-ion reactions and CID experiments and contributed to manuscript preparation. A.J.C. and S.A.M. contributed to the project design, interpretation of data and writing of the manuscript; R.A.J.O. devised the project, contributed to the design of experiments and interpretation of data, project management and writing of the manuscript.

## Conflicts of interest

"There are no conflicts to declare".

## Acknowledgements

We thank Dr. Joseph Bungard, Ph.D. for the synthesis of TMPDA. We acknowledge the support of the National Computing Infrastructure. WAOA thanks Prince Sattam Bin Abdulaziz University for the award of a Ph.D. scholarship. KCF and SAM acknowledge support from the National Science Foundation NSF CHE-2304386 and Sciex for its role in enabling instrumentation for executing ion-ion reactions studies.

## Notes and references

1. Kagan, H.; Namy, J., Tetrahedron report number 213: Lanthanides in organic synthesis. *Tetrahedron* **1986,** *42* (24), 6573-6614.
2. Molander, G. A., Application of lanthanide reagents in organic synthesis. *Chem. Rev.* **1992,** *92* (1), 29-68.
3. Bousrez, G.; Jaroschik, F., Organic synthesis with elemental lanthanides–going beyond samarium and ytterbium. *EurJOC* **2022,** *2022* (18), e202200202.
4. Sun, C.; Li, K.; Xue, D., Searching for novel materials via 4f chemistry. *J. Rare Earths* **2019,** *37* (1), 1-10.
5. Evans, D.; Fazakerley, G.; Phillips, R., Organometallic compounds of bivalent ytterbium. *J. Chem. Soc. D* **1970,** (4), 244-244.
6. Evans, D.; Fazakerley, G.; Phillips, R., Organometallic compounds of bivalent europium, ytterbium, and samarium. *J. Chem. Soc. A* **1971**, 1931-1934.
7. Wiecko, M.; Deacon, G. B.; Junk, P. C., Organolanthanoid-halide synthons—a new general route to monofunctionalized lanthanoid (ii) compounds? *Chem. Commun.* **2010,** *46* (28), 5076-5078.
8. Ali, S. H.; Deacon, G. B.; Junk, P. C.; Hamidi, S.; Wiecko, M.; Wang, J., Lanthanoid Pseudo-Grignard Reagents: A Major Untapped Resource. *Eur. J. Chem.* **2018,** *24* (1), 230-242.

9. Cotton, S., Aspects of the lanthanide-carbon σ-bond. *Coord. Chem. Rev.* **1997,** *160*, 93-127.
10. Zimmermann, M.; Anwander, R., Homoleptic rare-earth metal complexes containing Ln− C σ-bonds. *Chem. Rev.* **2010,** *110* (10), 6194-6259.
11. Ortu, F., Rare earth starting materials and methodologies for synthetic chemistry. *Chem. Rev.* **2022,** *122* (6), 6040-6116.
12. Rasmussen, S. C., Transmetalation: a fundamental organometallic reaction critical to synthesis and catalysis. *ChemTexts* **2020,** *7* (1), 1.
13. Wittig, G., The rôle of ate complexes as reaction-determining intermediates. *Quarterly Reviews, Chemical Society* **1966,** *20* (2), 191-210.
14. Cotton, S.; Hart, F.; Hursthouse, M.; Welch, A., Preparation and molecular structure of a σ-bonded lanthanide phenyl. *J. Chem. Soc., Chem. Commun.* **1972,** (22), 1225-1226.
15. Chan, H.-S.; Yang, Q.; Mak, T. C.; Xie, Z., Anionic dichlorolanthanocene compounds. X-ray crystal structures of [{(Me3Si) 2C5H3} 2LnCl2][Li (THF) 4](Ln= Er, Yb) and {(Me3Si) 2C5H3} 2Yb (μ-Cl) 2Li (THF) 2. *J. Organomet. Chem.* **2000,** *601* (1), 160-163.
16. Hitchcock, P. B.; Lappert, M. F.; Prashar, S., Syntheses and crystal structures of two ytterbocene complexes [Yb (η-Cp'') 2I (THF)] and [Yb (η-Cp'') 2 (μ-Cl) 2Li (THF) 2](Cp''= C5H3 (SiMe3) 2-1, 3). *J. Organomet. Chem.* **2000,** *613* (1), 105-110.
17. Imamoto, T.; Kusumoto, T.; Tawarayama, Y.; Sugiura, Y.; Mita, T.; Hatanaka, Y.; Yokoyama, M., Carbon-carbon bond-forming reactions using cerium metal or organocerium (III) reagents. *J. Org. Chem* **1984,** *49* (21), 3904-3912.
18. Molander, G. A.; Burkhardt, E. R.; Weinig, P., Diastereoselective addition of organoytterbium reagents to carbonyl substrates. *J. Org. Chem* **1990,** *55* (17), 4990-4991.
19. Sada, M.; Matsubara, S., Transition-metal chloride mediated addition reaction of diorganomagnesium to easily enolizable ketones. *Tetrahedron* **2011,** *67* (14), 2612-2616.
20. Packard, E.; Pascoe, D. D.; Maddaluno, J.; Gonçalves, T. P.; Harrowven, D. C., Organoytterbium ate complexes extend the value of cyclobutenediones as isoprene equivalents. *Angew. Chem.* **2013,** *125* (49), 13314-13317.
21. Partyka, D. V., Transmetalation of unsaturated carbon nucleophiles from boron-containing species to the mid to late d-block metals of relevance to catalytic C− X coupling reactions (X= C, F, N, O, Pb, S, Se, Te). *Chem. Rev.* **2011,** *111* (3), 1529-1595.
22. Deacon, G. B.; Evans, D. J.; Forsyth, C. M.; Junk, P. C., Lanthanoid (II) tetraphenylborate complexes: From discrete ions to pseudo metallocenes. *Coord. Chem. Rev.* **2007,** *251* (13-14), 1699-1706.
23. Deacon, G. B.; Forsyth, C. M., Synthesis and structures of the first cationic perfluoroaryllanthanoid (II) complexes. *Eur. J. Chem.* **2004,** *10* (7), 1798-1804.
24. Deacon, G. B.; Forsyth, C. M., Linkage isomerism and C–H activation in an ytterbium (ii) tetraphenylborate. *Chem. Commun.* **2002,** (21), 2522-2523.
25. Deacon, G. B.; Forsyth, C. M.; Junk, P. C., η6: η6 Coordination of Tetraphenylborate to Ytterbium (ii): A New Class of Lanthanoid ansa-Metallocenes. Eur. J. Inorg. Chem: Eur. J. Inorg. Chem, 2005.
26. Evans, W. J.; Walensky, J. R.; Furche, F.; DiPasquale, A. G.; Rheingold, A. L., Trigonal-Planar versus Pyramidal Geometries in the Tris (ring) Heteroleptic Divalent Lanthanide Complexes (C5Me5) Ln (μ-η6: η1-Ph) 2BPh2: Crystallographic and Density Functional Theory Analysis. *Organometallics* **2009,** *28* (20), 6073-6078.
27. Auth, T.; Koszinowski, K.; O'Hair, R. A., Dissecting Transmetalation Reactions at the Molecular Level: Phenyl Transfer in Metal Borate Complexes. *Organometallics* **2019,** *39* (1), 25-33.
28. Bathie, F.; Stewart, A. W.; Canty, A. J.; Richard, A., Dissecting transmetalation reactions at the molecular level: C–B versus F–B bond activation in phenyltrifluoroborate silver complexes. *Dalton Trans.* **2021,** *50* (4), 1496-1506.
29. Stewart, A. W.; Ma, H. Z.; Weragoda, G. K.; Khairallah, G. N.; Canty, A. J.; O'Hair, R. A., Dissecting transmetalation reactions at the molecular level: role of the coordinated anion in gas-phase models for the transmetalation step of the Hiyama cross-coupling reaction. *Organometallics* **2021,** *40* (12), 1822-1829.
30. Prentice, B. M.; McLuckey, S. A., Gas-phase ion/ion reactions of peptides and proteins: acid/base, redox, and covalent chemistries. *Chem. Commun.* **2013,** *49* (10), 947-965.
31. Foreman, D. J.; McLuckey, S. A., Recent developments in gas-phase ion/ion reactions for analytical mass spectrometry. *Anal. Chem.* **2019,** *92* (1), 252-266.
32. Fabijanczuk, K. C.; Altalhi, W. A.; Aldajani, A. M.; Canty, A. J.; McLuckey, S. A.; Richard, A., Ion-pairs as a gateway to transmetalation: aryl transfer from boron to nickel and magnesium. *Dalton Trans.* **2022,** *51* (14), 5699-5705.
33. Renaud, F.; Piguet, C.; Bernardinelli, G.; Bünzli, J. C. G.; Hopfgartner, G., In Search for Mononuclear Helical Lanthanide Building Blocks with Predetermined Properties: Triple-stranded Helical Complexes with N, N, N', N'-tetraethylpyridine-2, 6-dicarboxamide. *Eur. J. Chem.* **1997,** *3* (10), 1646-1659.
34. Hua, K. T.; Xu, J.; Quiroz, E. E.; Lopez, S.; Ingram, A. J.; Johnson, V. A.; Tisch, A. R.; de Bettencourt-Dias, A.; Straus, D. A.; Muller, G., Structural and photophysical properties of visible-and near-IR-emitting tris lanthanide (III) complexes formed with the enantiomers of N, N'-bis (1-phenylethyl)-2, 6-pyridinedicarboxamide. *Inorg. Chem.* **2012,** *51* (1), 647-660.

35. Chen, X.; Xiong, Z.; Gong, Y., Complexation of Ln3+ with Pyridine-2, 6-dicarboxamide: Formation of the 1: 2 Complexes in Solution and Gas Phase. *Inorg. Chem.* **2020,** *59* (19), 14486-14492.
36. Alyapyshev, M. Y.; Babain, V.; Tkachenko, L.; Eliseev, I.; Didenko, A.; Petrov, M., Dependence of extraction properties of 2, 6-dicarboxypyridine diamides on extractant structure. *Solvent Extr. Ion Exch.* **2011,** *29* (4), 619-636.
37. Bhanot, J. S.; Fabijanczuk, K. C.; Abdillahi, A. M.; Chao, H.-C.; Pizzala, N. J.; Londry, F. A.; Dziekonski, E. T.; Hager, J. W.; McLuckey, S. A., Adaptation and operation of a quadrupole/time-of-flight tandem mass spectrometer for high mass ion/ion reaction studies. *Int. J. Mass Spectrom.* **2022,** *478*, 116874.
38. Xia, Y.; Liang, X.; McLuckey, S. A., Pulsed dual electrospray ionization for In/In reactions. *J. Am. Soc. Mass Spectrom.* **2005,** *16* (11), 1750-1756.
39. Wells, J. M.; McLuckey, S. A., Collision-induced dissociation (CID) of peptides and proteins. *Meth. Enzymol.* **2005,** *402*, 148-185.
40. M. J. Frisch, G. W. T., H. B. Schlegel, G. E. Scuseria, M. A. Robb, J. R. Cheeseman, G. Scalmani, V. Barone, G. A. Petersson, H. Nakatsuji, X. Li, M. Caricato, A. V. Marenich, J. Bloino, B. G. Janesko, R. Gomperts, B. Mennucci, H. P. Hratchian, J. V. Ortiz, A. F. Izmaylov, J. L. Sonnenberg, D. Williams Young, F. Ding, F. Lipparini, F. Egidi, J. Goings, B. Peng, A. Petrone, T. Henderson, D. Ranasinghe, V. G. Zakrzewski, J. Gao, N. Rega, G. Zheng, W. Liang, M. Hada, M. Ehara, K. Toyota, R. Fukuda, J. Hasegawa, M. Ishida, T. Nakajima, Y. Honda, O. Kitao, H. Nakai, T. Vreven, K. Throssell, J. A. Montgomery Jr., J. E. Peralta, F. Ogliaro, M. J. Bearpark, J. J. Heyd, E. N. Brothers, K. N. Kudin, V. N. Staroverov, T. A. Keith, R. Kobayashi, J. Normand, K. Raghavachari, A. P. Rendell, J. C. Burant, S. S. Iyengar, J. Tomasi, M. Cossi, J. M. Millam, M. Klene, C. Adamo, R. Cammi, J. W. Ochterski, R. L. Martin, K. Morokuma, O. Farkas, J. B. Foresman and D. J. Fox, Gaussian 16, Revision C.01, Gaussian, Inc., Wallingford CT, 2019.
41. Zhao, Y.; Truhlar, D. G., The M06 suite of density functionals for main group thermochemistry, thermochemical kinetics, noncovalent interactions, excited states, and transition elements: two new functionals and systematic testing of four M06-class functionals and 12 other functionals. *Theor. Chem. Acc.* **2008,** *120*, 215-241.
42. Pracht, P.; Bohle, F.; Grimme, S., Automated exploration of the low-energy chemical space with fast quantum chemical methods. *Phys. Chem. Chem. Phys.* **2020,** *22* (14), 7169-7192.
43. Bannwarth, C.; Ehlert, S.; Grimme, S., GFN2-xTB—An accurate and broadly parametrized self-consistent tight-binding quantum chemical method with multipole electrostatics and density-dependent dispersion contributions. *J. Chem. Theory Comput.* **2019,** *15* (3), 1652-1671.
44. Eckelmann, J.; Saggiomo, V.; Sönnichsen, F. D.; Lüning, U., The first supramolecular ion triplet complex. *New Journal of Chemistry* **2010,** *34* (7), 1247-1250.
45. Kepp, K. P., A Quantitative Scale of Oxophilicity and Thiophilicity. *Inorg Chem* **2016,** *55* (18), 9461-70.
46. Deacon, G. B.; Forsyth, C. M.; Freckmann, D.; Junk, P. C.; Konstas, K.; Luu, J.; Meyer, G.; Werner, D., Adventitiously Obtained Rare-Earth Peroxide Complexes and Their Structural Characterisation. *Australian Journal of Chemistry* **2014,** *67* (12), 1860-1865.
47. Patroniak, V.; Kubicki, M.; Mondry, A.; Lisowski, J.; Radecka-Paryzek, W., Pentaaza macrocyclic ytterbium(iii) complex and solvent controlled supramolecular self-assembly of its dimeric μ-η2:η2 peroxo-bridged derivatives. *Dalton Transactions* **2004,** (20), 3295-3304.
48. Niemeyer, M., Synthesis and Structural Characterization of Several Ytterbium Bis(trimethylsilyl)amides Including Base-free [Yb{N(SiMe3)2}2(μ-Cl)]2 — A Coordinatively Unsaturated Complex with Additional Agostic Yb···(H3C—Si) Interactions. *Zeitschrift für anorganische und allgemeine Chemie* **2002,** *628* (3), 647-657.
49. Fielicke, A., Probing the binding and activation of small molecules by gas-phase transition metal clusters via IR spectroscopy. *Chemical Society Reviews* **2023,** *52* (11), 3778-3841.